

ACQUIRED CLUSTERING PROPERTIES AND SOLUTION OF CERTAIN SADDLE POINT SYSTEMS *

M.A. OLSHANSKII [†] AND V. SIMONCINI[‡]

Abstract. Many mathematical models involve flow equations characterized by nonconstant viscosity, and a Stokes type problem with variable viscosity coefficient arises. Appropriate block diagonal preconditioners for the resulting algebraic saddle point linear system produce well clustered spectra, except for a few interior isolated eigenvalues which may tend to approach zero. These outliers affect the convergence of Krylov subspace system solvers, causing a possibly long stagnation phase. In this paper we characterize the influence of the spectral properties of the preconditioner on the final spectrum of the saddle point matrix, by providing accurate spectral intervals depending on the involved operators. Moreover, we suggest that the stagnation phase may be completely eliminated by means of an augmentation procedure, where approximate spectral eigenspace information can be injected. We show that the modifications to the original code are minimal and can be easily implemented. Numerical experiments confirm our findings.

Key words. saddle-point problem, preconditioning, eigenvalue clusterings, outliers, varying viscosity

AMS subject classifications. 65F10, 65F15, 65N22, 76D07

1. Introduction. Many mathematical models involve flow equations characterized by nonconstant viscosity. They occur, for example, in geophysical and convection flows, where the viscosity is a function of the temperature (see, e.g., [8, 27]), or in quasi-Newtonian (non-Newtonian) fluids motion modeling, where the viscosity may depend on the second invariant of the rate deformation tensor and the pressure [14]. If inertia phenomena are neglected (creeping flows) and/or a linearization is applied to these models, the following Stokes type problem with variable viscosity coefficient arises:

$$\begin{aligned} -\operatorname{div}\nu(\mathbf{x})\mathbf{D}\mathbf{u} + \nabla p &= \mathbf{f} && \text{on } \Omega, \\ -\operatorname{div} \mathbf{u} &= 0 && \text{on } \Omega, \\ \mathbf{u} &= 0 && \text{on } \partial\Omega, \end{aligned} \tag{1.1}$$

with $0 < \nu_{\min} \leq \nu(\mathbf{x}) \leq \nu_{\max} < \infty$. Here \mathbf{u} denotes the velocity vector field, p is the pressure; $\mathbf{D}\mathbf{u} = \frac{1}{2}(\nabla\mathbf{u} + \nabla^T\mathbf{u})$ is the rate of the deformation tensor, Ω is a bounded domain in \mathbb{R}^d .

A stable finite element or finite difference method applied to discretize (1.1) leads to the solution of the following so-called saddle point linear system

$$\begin{cases} Ax + B^T y = f \\ Bx = 0 \end{cases} \quad \text{or} \quad \mathcal{A}u = b, \tag{1.2}$$

with $A \in \mathbb{R}^{n \times n}$ and $B \in \mathbb{R}^{m \times n}$, $m \leq n$. Since the pressure p is defined up to a constant, the matrix B is one-rank deficient. Correspondingly, if y is sought from appropriate subspace of \mathbb{R}^m then (1.2) has a unique solution. For the clearness of

*Version of 15 April 2010.

[†]Department of Mechanics and Mathematics, M.V. Lomonosov Moscow State University, Moscow 119899, Russia (Maxim.Olshanskii@mtu-net.ru); This work was supported by the Russian Foundation for Basic Research through projects 09-01-00115 and 08-01-00159

[‡]Dipartimento di Matematica, Università di Bologna, Piazza di Porta S. Donato 5, I-40127 Bologna, Italy and CIRSA, Ravenna, Italy (valeria@dm.umibo.it).

presentation we assume in sections 2–3 that B has a full rank and \mathcal{A} is nonsingular. In this example, A is a symmetric positive definite sparse matrix, corresponding to the diffusion vector problem. Effective preconditioning techniques try to exploit the block form of the system; see, e.g. [2] for a general discussion on structured preconditioners for this problem. We consider the following block diagonal preconditioner

$$\mathcal{P} = \begin{bmatrix} P & 0 \\ 0 & S \end{bmatrix}, \quad (1.3)$$

where P and S are symmetric positive definite matrices, suitably chosen so that $P \approx A$ and $S \approx BA^{-1}B^T$. In the literature one can find geometric or algebraic multigrid (see, e.g., [12, 20]) or domain decomposition [18, 28] iterative algorithms which provide effective preconditioners P for matrix A if the function ν is sufficiently regular. Other options to build P include the use of incomplete factorizations or approximate inverses; see, e.g., [1]. The appropriate and natural choice for the preconditioner S is the pressure mass matrix with respect to the weighted scalar product $(\nu^{-1}\cdot, \cdot)_{L^2(\Omega)}$ (finite elements) or $S = \text{diag}\{\nu^{-1}(\mathbf{x}_i)\}$ (finite differences, with \mathbf{x}_i for i -th pressure grid node), cf. [6, 10, 11, 15, 19]. In many cases, such choice of S leads to a well clustered spectrum of the preconditioned Schur complement matrix $BA^{-1}B^TS^{-1}$. However, there are situations (cf. section 4) when the eigenvalues of $BA^{-1}B^TS^{-1}$ are well clustered except for few small outliers.

In this paper we show how the eigenvalue distribution of the preconditioned Schur complement matrix, and in particular the presence of outliers, is accurately inherited by the coupled preconditioned matrix $\mathcal{A}\mathcal{P}^{-1}$. Although this particular spectral distribution frequently occurs when S is a *quasi*-optimal preconditioner for the Schur complement, its effects on the spectrum of $\mathcal{A}\mathcal{P}^{-1}$ do not appear to have been investigated in the literature. We aim to fill this gap by deriving refined spectral intervals for $\mathcal{A}\mathcal{P}^{-1}$ which highlight the role of all involved matrices (cf. section 2).

In general, the most visible effect of a small number of outliers on the convergence history of the system solver is a stagnation phase. Based on our spectral analysis, we show that approximate spectral information associated with the outliers can be very effectively injected during the approximation by means of a Krylov subspace minimal residual method. More precisely, we shall employ augmentation with deflation (see, e.g., the general presentation in [25]), which requires minimal modifications to the original algorithm (cf. section 3).

Further in section 4, we consider one particular application in the field of numerical visco-plasticity to show the occurrence of outliers in the spectrum. Finally in section 5, the theory is illustrated by numerical experiments.

2. The analysis. We analyze the spectral properties of the preconditioned linear system with coefficient matrix $\mathcal{A}\mathcal{P}^{-1}$. Let $0 < \lambda_1 \leq \dots \leq \lambda_n$ be the eigenvalues of AP^{-1} , and let $0 < \mu_1 \leq \dots \leq \mu_m$ be the eigenvalues of $BA^{-1}B^TS^{-1}$. For the latter we assume the following clustering property: With some ℓ , $0 < \ell < m$, it holds

$$\mu_\ell \leq \varepsilon_0 \quad \text{and} \quad \mu_{\ell+1} > c_0. \quad (2.1)$$

Specifically, we focus on the case when $\varepsilon_0 \ll c_0$ and $\ell \ll m$. Consider the generalized eigenvalue problem

$$\mathcal{A}z = \lambda \mathcal{P}z. \quad (2.2)$$

We are interested in the analysis of (2.2) when the preconditioned Schur complement shows a strong clustering of eigenvalues, together with a few outlying eigenvalues close

to zero, i.e. property (2.1). To this end, consider the equivalent eigenvalue problem by setting $w = \mathcal{P}^{\frac{1}{2}}z$ and $\tilde{\mathcal{A}} = \mathcal{P}^{-\frac{1}{2}}\mathcal{A}\mathcal{P}^{-\frac{1}{2}}$:

$$\tilde{\mathcal{A}}w = \lambda w, \quad \text{with} \quad \tilde{\mathcal{A}} = \begin{bmatrix} \tilde{A} & \tilde{B}^T \\ \tilde{B} & 0 \end{bmatrix},$$

where, clearly, $\tilde{A} = P^{-\frac{1}{2}}AP^{-\frac{1}{2}}$ and $\tilde{B} = S^{-\frac{1}{2}}BP^{-\frac{1}{2}}$. We start with a lemma describing the spectral distribution of the matrix $\tilde{B}\tilde{B}^T = S^{-\frac{1}{2}}BP^{-1}B^TS^{-\frac{1}{2}}$ in terms of that of $S^{-\frac{1}{2}}BA^{-1}B^TS^{-\frac{1}{2}}$.

LEMMA 2.1. *Let the eigenvalues of $BA^{-1}B^TS^{-1}$ and of $BP^{-1}B^TS^{-1}$ be ordered increasingly. Then we have*

$$\lambda_1\mu_j \leq \lambda_j(BP^{-1}B^TS^{-1}) \leq \lambda_n\mu_j.$$

Proof. We can write $A^{-\frac{1}{2}}B^TS^{-\frac{1}{2}} = (A^{-\frac{1}{2}}P^{\frac{1}{2}})P^{-\frac{1}{2}}B^TS^{-\frac{1}{2}}$. Analogously, we have $P^{-\frac{1}{2}}B^TS^{-\frac{1}{2}} = (P^{-\frac{1}{2}}A^{\frac{1}{2}})A^{-\frac{1}{2}}B^TS^{-\frac{1}{2}}$. Using standard singular value inequalities (see, e.g., [13, Th.3.3.16]) we have

$$\sigma_i(P^{-\frac{1}{2}}B^TS^{-\frac{1}{2}}) \leq \|P^{-\frac{1}{2}}A^{\frac{1}{2}}\| \sigma_i(A^{-\frac{1}{2}}B^TS^{-\frac{1}{2}})$$

and

$$\sigma_i(A^{-\frac{1}{2}}B^TS^{-\frac{1}{2}}) \leq \|A^{-\frac{1}{2}}P^{\frac{1}{2}}\| \sigma_i(P^{-\frac{1}{2}}B^TS^{-\frac{1}{2}}),$$

where $\sigma_i(X)$ denotes the i th singular value of X , decreasingly ordered. Recalling that $\mu_{m-i+1}(BA^{-1}B^TS^{-1}) = \sigma_i(A^{-\frac{1}{2}}B^TS^{-\frac{1}{2}})^2$ and that $\lambda_{m-i+1}(BP^{-1}B^TS^{-1}) = \sigma_i(P^{-\frac{1}{2}}B^TS^{-\frac{1}{2}})^2$, the result follows. \square

Let $\Theta > 0$ be the diagonal matrix of eigenvalues of $BP^{-1}BS^{-1}$ or, equivalently, of $\tilde{B}\tilde{B}^T$. The previous lemma shows that if the eigenvalues of AP^{-1} do not significantly deviate from one, that is P is a good preconditioner for A , then the clustering properties of $\text{spec}(BA^{-1}B^TS^{-1})$ are inherited by $\text{spec}(BP^{-1}B^TS^{-1})$. In light of this we consider the decomposition $\Theta = \text{blkdiag}(\Theta_1, \Theta_2)$ where $\Theta_1 > c_0\lambda_1$ and $\Theta_2 \leq \varepsilon$, with some $\varepsilon \leq \varepsilon_0\lambda_n$. In particular, we can also assume that the dimensions of the two blocks Θ_i , $i = 1, 2$ are ℓ and $m - \ell$, respectively. Let

$$\tilde{B}^T = [U_1, U_2] \begin{bmatrix} \Theta_1^{\frac{1}{2}} & \\ & \Theta_2^{\frac{1}{2}} \end{bmatrix} V^T$$

be the skinny singular value decomposition of \tilde{B}^T , so that $[U_1, U_2]$ is rectangular. Then we can write the eigenvalue problem $\tilde{\mathcal{A}}w = \lambda w$ as¹

$$\left[\begin{array}{cc|c} \tilde{A} & U_1\Theta_1^{\frac{1}{2}} & U_2\Theta_2^{\frac{1}{2}} \\ \hline \Theta_1^{\frac{1}{2}}U_1^T & 0 & 0 \\ \Theta_2^{\frac{1}{2}}U_2^T & 0 & 0 \end{array} \right] u = \lambda u, \quad \text{with} \quad u = \begin{bmatrix} I_n & \\ & V^T \end{bmatrix} w.$$

¹We recall that in some applications B could be rank deficient. The proposed formulation could still be exploited by using the decomposition $\tilde{B}^T = [U_1, U_2, U_3] = \text{blockdiag}(\Theta_1^{\frac{1}{2}}, \Theta_2^{\frac{1}{2}}, 0)V^T$, and then restricting the analysis to the first two block rows and columns of $\tilde{\mathcal{A}}$. Since the subsequent steps would be the same, we directly work with the full rank case, while keeping in mind the extra zero columns and rows in $\tilde{\mathcal{A}}$ if needed.

We define

$$\widetilde{\mathcal{M}} = \begin{bmatrix} \tilde{\mathcal{A}} & U_1 \Theta_1^{\frac{1}{2}} & 0 \\ \Theta_1^{\frac{1}{2}} U_1^T & 0 & 0 \\ 0 & 0 & 0 \end{bmatrix} =: \begin{bmatrix} \mathcal{M} & \\ & 0 \end{bmatrix}$$

with $\text{spec}(\widetilde{\mathcal{M}}) = \text{spec}(\mathcal{M}) \cup \{0\}$, so that

$$\tilde{\mathcal{A}} = \widetilde{\mathcal{M}} + \mathcal{E}.$$

The eigenvalues of the ‘‘perturbation’’ matrix \mathcal{E} can be bounded as follows.

LEMMA 2.2. *With the previous notation,*

$$\text{spec}(\mathcal{E}) \subseteq [-\|\Theta_2\|^{\frac{1}{2}}, \|\Theta_2\|^{\frac{1}{2}}] \subseteq [-\varepsilon^{\frac{1}{2}}, \varepsilon^{\frac{1}{2}}].$$

We next use the decomposition of $\tilde{\mathcal{A}}$ and Lemma 2.2 to derive estimates for the spectral interval of $\tilde{\mathcal{A}}$ as a perturbation of the spectral interval of $\widetilde{\mathcal{M}}$.

Since the matrix \mathcal{M} is once again in saddle point form, well known results ([21]) provide sharp estimates for its spectral interval. Let $\theta_{\max}^{(i)}$, $\theta_{\min}^{(i)}$ be the largest and smallest diagonal values of Θ_i , that is $\sqrt{\theta_{\max}^{(i)}}$, $\sqrt{\theta_{\min}^{(i)}}$ are the largest and smallest nonzero singular values of $U_i \Theta_i^{\frac{1}{2}}$. Then it holds:

$$\begin{aligned} \text{spec}(\mathcal{M}) \subseteq & \left[\frac{1}{2} \left(\lambda_1 - \sqrt{\lambda_1^2 + 4\theta_{\max}^{(1)}} \right), \frac{1}{2} \left(\lambda_n - \sqrt{\lambda_n^2 + 4\theta_{\min}^{(1)}} \right) \right] \\ & \cup \left[\lambda_1 \frac{1}{2} \left(\lambda_n + \sqrt{\lambda_n^2 + 4\theta_{\max}^{(1)}} \right) \right], \end{aligned} \quad (2.3)$$

where the first interval is negative and the second one is positive.

We next recall in our notation a perturbation bound due to Weyl; see, e.g., [26].

THEOREM 2.3. *Let $\tilde{\mathcal{A}} = \widetilde{\mathcal{M}} + \mathcal{E}$, and assume all eigenvalues are sorted in decreasing order. Then*

$$\lambda_i(\tilde{\mathcal{A}}) \in [\lambda_i(\widetilde{\mathcal{M}}) + \lambda_{\min}(\mathcal{E}), \lambda_i(\widetilde{\mathcal{M}}) + \lambda_{\max}(\mathcal{E})]$$

We thus get the following bound for the eigenvalues of (2.2).

LEMMA 2.4. *With the previous notation,*

$$\begin{aligned} \text{spec}(\tilde{\mathcal{A}}) \subseteq & \left[\frac{1}{2} \left(\lambda_1 - \sqrt{\lambda_1^2 + 4\theta_{\max}^{(1)}} \right), \frac{1}{2} \left(\lambda_n - \sqrt{\lambda_n^2 + 4\theta_{\min}^{(1)}} \right) + \varepsilon^{\frac{1}{2}} \right] \\ & \cup \left[\lambda_1, \frac{1}{2} \left(\lambda_n + \sqrt{\lambda_n^2 + 4\theta_{\max}^{(1)}} \right) \right] \cup \left[-\varepsilon^{\frac{1}{2}}, \lambda_n - \sqrt{\lambda_n^2 + 4\theta_{\min}^{(2)}} \right] \end{aligned}$$

Moreover, for sufficiently small ε at most ℓ eigenvalues of $\tilde{\mathcal{A}}$ are in the interval $\left[-\varepsilon^{\frac{1}{2}}, \lambda_n - \sqrt{\lambda_n^2 + 4\theta_{\min}^{(2)}} \right]$.

Proof. Applying Theorem 2.3, Lemma 2.2, (2.3) and recalling that $\text{spec}(\widetilde{\mathcal{M}}) = \text{spec}(\mathcal{M}) \cup \{0\}$, we get the following bounds

$$\begin{aligned} \text{spec}(\tilde{\mathcal{A}}) \subseteq & \left[\frac{1}{2} \left(\lambda_1 - \sqrt{\lambda_1^2 + 4\theta_{\max}^{(1)}} \right) - \varepsilon^{\frac{1}{2}}, \frac{1}{2} \left(\lambda_n - \sqrt{\lambda_n^2 + 4\theta_{\min}^{(1)}} \right) + \varepsilon^{\frac{1}{2}} \right] \\ & \cup \left[\lambda_1 - \varepsilon^{\frac{1}{2}}, \frac{1}{2} \left(\lambda_n + \sqrt{\lambda_n^2 + 4\theta_{\max}^{(1)}} \right) + \varepsilon^{\frac{1}{2}} \right] \cup \left[-\varepsilon^{\frac{1}{2}}, \varepsilon^{\frac{1}{2}} \right]. \end{aligned} \quad (2.4)$$

Since 0 is the eigenvalue of multiplicity ℓ for \mathcal{M} , at most ℓ eigenvalues of $\tilde{\mathcal{A}}$ are in the third interval if there is no intersection with the first interval. The latter holds for sufficiently small ε such that $4\varepsilon^{\frac{1}{2}} < \sqrt{\lambda_n^2 + 4\theta_{\min}^{(1)}} - \lambda_n$. Further, the standard estimates ([21]) imply

$$\begin{aligned} \text{spec}(\tilde{\mathcal{A}}) \subseteq & \left[\frac{1}{2} \left(\lambda_1 - \sqrt{\lambda_1^2 + 4\theta_{\max}^{(1)}} \right), \frac{1}{2} \left(\lambda_n - \sqrt{\lambda_n^2 + 4\theta_{\min}^{(2)}} \right) \right] \\ & \cup \left[\lambda_1, \frac{1}{2} \left(\lambda_n + \sqrt{\lambda_n^2 + 4\theta_{\max}^{(1)}} \right) \right]. \end{aligned}$$

The intersection of (2.4) and (2.5) yields the result. \square

Since the clustering property of the modified preconditioned Schur complement is tightly related to that of the original preconditioned Schur complement, the spectral intervals can be written in terms of the latter one, yielding our main result.

THEOREM 2.5. *Let $0 < \lambda_1 \leq \dots \leq \lambda_n$ be the eigenvalues of AP^{-1} , and let $0 < \mu_1 \leq \dots \leq \mu_m$ be the eigenvalues of $BA^{-1}B^TS^{-1}$ and assume that (2.1) holds. The following inclusion holds*

$$\begin{aligned} \text{spec}(\tilde{\mathcal{A}}) \subseteq & \left[\frac{1}{2} \left(\lambda_1 - \sqrt{\lambda_1^2 + 4\lambda_n\mu_m} \right), \frac{1}{2} \left(\lambda_n - \sqrt{\lambda_n^2 + 4\lambda_1\mu_{\ell+1}} \right) + (\varepsilon_0\lambda_n)^{\frac{1}{2}} \right] \\ & \cup \left[\lambda_1, \frac{1}{2} \left(\lambda_n + \sqrt{\lambda_n^2 + 4\lambda_n\mu_m} \right) \right] \cup \left[-(\varepsilon_0\lambda_n)^{\frac{1}{2}}, \lambda_n - \sqrt{\lambda_n^2 + 4\lambda_1\mu_1} \right] \end{aligned}$$

For sufficiently small ε_0 at most ℓ eigenvalues of $\tilde{\mathcal{A}}$ are in the third interval.

Proof. From Lemma 2.1 we know that $\theta_j^{(i)} \leq \lambda_n\mu_j^{(i)}$ and $\theta_j^{(i)} \geq \lambda_1\mu_j^{(i)}$, $j = 1, \dots, m$. The proof follows from substituting these inequalities in the bounds of Theorem 2.4 and recalling that $\varepsilon \leq \varepsilon_0\lambda_n$. \square

Theorem 2.5 shows that if the eigenvalues of AP^{-1} are well clustered, and if the eigenvalues of the preconditioned Schur complement satisfy (2.1), then most eigenvalues of the preconditioned saddle point matrix are contained in the first two intervals, of small size and away from zero, whereas only at most ℓ eigenvalues may approach zero, in a way that depends on the magnitude of the eigenvalues in μ_k , with $k \leq \ell$. In particular, for $\varepsilon_0 \rightarrow 0$, the right extreme of the interval $\left[-(\varepsilon_0\lambda_n)^{\frac{1}{2}}, \lambda_n - \sqrt{\lambda_n^2 + 4\lambda_1\mu_1} \right]$ behaves like $-\mu_1$, with $\mu_1 \leq \varepsilon_0$.

It is also important to realize that the clustering of the remaining eigenvalues strongly depends on the quality of the employed preconditioner. Thus if P is a poor approximation to A , then, say, small positive eigenvalues may still arise; One such example is reported in section 5.

REMARK 2.6. In terms of eigenvalues of AP^{-1} and $BA^{-1}B^TS^{-1}$ the upper bound for the negative part of $\text{spec}(\tilde{\mathcal{A}})$ can be slightly improved (cf. [24], eq. (2.18)). Thus the third interval from theorem 2.5 can be changed to $\left[-(\varepsilon_0\lambda_n)^{\frac{1}{2}}, \lambda_1 - \sqrt{\lambda_1^2 + 4\lambda_1\mu_1} \right]$. However, we do not see a direct argument enabling us to improve accordingly the upper bound in the first interval from Theorem 2.5.

3. Augmented Krylov subspace solver. Let $\mathcal{P} = LL^T$ be the Cholesky factorization of the preconditioner, and let $\hat{\mathcal{A}} = L^{-1}\mathcal{A}L^{-T}$ be the symmetrically preconditioned matrix. We are thus lead to solve the following symmetric indefinite system

$$\hat{\mathcal{A}}\hat{u} = \hat{b}, \quad \hat{b} = L^{-1}b, \quad u = L^{-T}\hat{u}, \quad (3.1)$$

by means of the Krylov subspace method MINRES (MINimal RESidual method), which minimizes the residual norm at each iteration. We next describe how (approximate) eigenspace information associated with outlying eigenvalues may be injected into the approximation space to possibly eliminate the stagnation phase caused by the outliers. The analysis in the previous section shows that for the considered problem an outlying set of eigenvalues may exist; moreover, due to the properties of the preconditioner, it is possible to identify the eigenspace responsible for the convergence delay and to construct an effective augmented approximation space; see section 5.

Our approach consists in judiciously augmenting the approximation space by including the approximate eigenspace. This procedure is inspired by that for the Conjugate Gradient algorithm in [23], although here an indefinite problem is considered, so that a different approximation strategy is required. We refer to [25] for a discussion on other augmentation and deflation strategies.

Assume that an approximation to an eigenspace of $\hat{\mathcal{A}}$ is available, and let the orthonormal columns of the matrix Y span such space. The augmented-deflated Lanczos algorithm builds a sequence $\{v_j\}$, $j = 1, 2, \dots$ of vectors such that

$$v_{j+1} \perp \text{span}\{Y, v_1, v_2, \dots, v_j\} \quad (3.2)$$

with $\|v_{j+1}\| = 1$; In the following we shall use $V_j := [v_1, \dots, v_j]$. To obtain such a sequence, we apply the standard Lanczos procedure, see, e.g., [9, 22], to the auxiliary matrix

$$\mathcal{G} := \hat{\mathcal{A}} - \hat{\mathcal{A}}Y(Y^T\hat{\mathcal{A}}Y)^{-1}Y^T\hat{\mathcal{A}},$$

with the initial vector given by $v_1 = r_0/\|r_0\|$, where $r_0 = \hat{b} - \hat{\mathcal{A}}\hat{u}_0$ is the residual associated with the starting approximation \hat{u}_0 . In case the matrix $Y^T\hat{\mathcal{A}}Y$ is singular, its pseudoinverse is used in place of the inverse². To ensure that v_1 is orthogonal to Y , we take as starting approximation

$$\hat{u}_0 = Y(Y^T\hat{\mathcal{A}}Y)^{-1}Y^T\hat{b}, \quad (3.3)$$

giving $Y^T r_0 = Y^T \hat{b} - Y^T \hat{\mathcal{A}} \hat{u}_0 = 0$. It can be shown by induction that $v_{j+1}^T Y = 0$ so that the obtained basis in (3.2) is indeed orthogonal. The computed augmented Krylov subspace is denoted by $K_j(\hat{\mathcal{A}}, Y, v_1)$. A Minimal Residual method determines an approximate solution $\hat{u}_j \in \hat{u}_0 + K_j(\hat{\mathcal{A}}, Y, v_1)$ by requiring that the residual $r_j = \hat{b} - \hat{\mathcal{A}}\hat{u}_j$ be orthogonal to $\mathcal{G}K_j(\hat{\mathcal{A}}, Y, v_1)$.

The following result shows how \hat{u}_j can be computed so as to obtain a residual minimizing approximate solution.

PROPOSITION 3.1. *Under the previous notation, let $\hat{u}_j = \hat{u}_0 + Yz_1 + V_j z_2$. If $z_1 = -(Y^T\hat{\mathcal{A}}Y)^{-1}Y^T\hat{\mathcal{A}}V_j z_2$, then*

$$\hat{b} - \hat{\mathcal{A}}\hat{u}_j \perp \mathcal{G}K_j(\hat{\mathcal{A}}, Y, v_1) \quad \text{iff} \quad z_2 = \arg \left(\min_{z \in \mathbb{R}^j} \|r_0 - \mathcal{G}V_j z\| \right).$$

Proof. Let $W_j = [Y, V_j]$, so that the columns of W_j span the Krylov subspace $K_j(\hat{\mathcal{A}}, Y, v_1)$, and let $\hat{u}_j = \hat{u}_0 + W_j \zeta = \hat{u}_0 + Yz_1 + V_j z_2$. We observe that $Y^T \mathcal{G} = 0$

²To cope with round-off errors, it is advisable to include the eigenvector corresponding to the zero eigenvalue. This is carried out by appropriately modifying the computed pseudoinverse.

by definition of \mathcal{G} , therefore it is sufficient to impose the condition on $\mathcal{G}V_j$. Using $z_1 = -(Y^T \widehat{\mathcal{A}}Y)^{-1}Y^T \widehat{\mathcal{A}}V_j z_2$, we have

$$0 = V_j^T \mathcal{G}r_j = V_j^T \mathcal{G}(r_0 - \widehat{\mathcal{A}}Y z_1 - \widehat{\mathcal{A}}V_j z_2) \quad (3.4)$$

$$= V_j^T \mathcal{G}(r_0 - (\widehat{\mathcal{A}} - \widehat{\mathcal{A}}Y(Y^T \widehat{\mathcal{A}}Y)^{-1}Y^T \widehat{\mathcal{A}})V_j z_2) = V_j^T \mathcal{G}(r_0 - \mathcal{G}V_j z_2), \quad (3.5)$$

which is the solution to the minimization problem $\min_{z \in \mathbb{R}^j} \|r_0 - \mathcal{G}V_j z\|$. \square

We stress that because the solution is approximated in the space generated by both Y and V_j , that is the components onto Y are not only simply deflated by using \mathcal{G} , it is not necessary that Y be an extremely good approximation to the critical eigenvectors. The inclusion of this information to the space appears to be beneficial even when augmentation is performed with rather poor eigenvector approximations.

Due to the preceding derivation, the changes to the standard MINRES code are minimal and they can be summarized as follows:

1. The initial approximation is given by (3.3);
2. The coefficient matrix is formally given by \mathcal{G} , so that matrix-vector products are computed as $\mathcal{G}v = \widehat{\mathcal{A}}v - \widehat{\mathcal{A}}Y(Y^T \widehat{\mathcal{A}}Y)^{-1}Y^T \widehat{\mathcal{A}}v$. To limit the number of matrix-vector multiplies with $\widehat{\mathcal{A}}$, the matrices $Y_1 = \widehat{\mathcal{A}}Y$ and $T = (Y^T \widehat{\mathcal{A}}Y)^{-1}$ could be explicitly computed and saved once for all at the beginning;
3. The regular approximate solution update $\hat{u}_{j+1} = \hat{u}_j + p_j a_j$ (see³, e.g., [9, Algorithm 4]) is modified as follows, to take into account the definition of z_1 in Proposition 3.1:

$$\hat{u}_{j+1} = \hat{u}_j + p_j a_j - Y(Y^T \widehat{\mathcal{A}}Y)^{-1}Y^T \widehat{\mathcal{A}}p_j a_j.$$

In many cases, symmetrically preconditioning the problem as in (3.1) may be unfeasible; this occurs for instance when Multigrid or Multilevel methods are used to approximate some of the relevant matrix blocks. In this case, a MINRES algorithm can be implemented that only requires solves with \mathcal{P} , rather than with its factors; see, e.g., [7, 16]. Corresponding modifications to the code may be included to ensure that the wanted space is deflated. A possible algorithm describing the whole procedure is given next. The presented version is based on a Matlab implementation of the MINRES code that can be found at

<http://www.stanford.edu/group/SOL/software/minres.html>

See also [7, 16]. The additional operations associated with augmentation are reported in bold face. Note that here, as opposed to the derivation in the symmetrized case, Y is an approximation to eigenvectors of $P^{-1}A$ to be deflated. If approximations Y_0 to selected eigenvectors of $L^{-1}AL^{-T}$ are available, then $Y = L^{-T}Y_0$ should be used.

Algorithm AUGMENTED MINRES

Given A, b , maxit, tol, P , and Y with orthonormal columns

$\mathbf{u} = \mathbf{Y}(\mathbf{Y}^T \mathcal{A} \mathbf{Y})^{-1} \mathbf{Y}^T \mathbf{b}$ starting approximation

$r = b - \mathcal{A}u$, $r_1 = r$, $y = P^{-1}r$

$\beta_1 = \sqrt{r^T y}$

$\beta = \beta_1$, $\beta_0 = 0$, $\bar{d} = 0$, $e = 0$, $\bar{\phi} = \beta_1$, $\chi_1 = \beta_1$, $\chi_2 = 0$

$c = -1$, $s = 0$, $i = 0$, $w = 0$, $w_2 = 0$, $r_2 = r_1$

while ($i < \text{maxit}$)

$i = i + 1$

³Note however a shift in the indexing for consistency with our notation.

$v = y/\beta;$
 $\mathbf{y} = \mathcal{A}\mathbf{v} - \mathcal{A}\mathbf{Y}(\mathbf{Y}^T\mathcal{A}\mathbf{Y})\mathbf{Y}^T\mathcal{A}\mathbf{v}$
 if $i \geq 2$, $y = y - (\beta/\beta_0)r_1$
 $\alpha = v^T y$
 $y = y - r_2\alpha/\beta$
 $r_1 = r_2, \quad r_2 = y$
 $y = P^{-1}r_2$
 $\beta_0 = \beta, \quad \beta = \sqrt{r_2^T y}$
 $e_0 = e, \quad \delta = c\bar{d} + s\alpha \quad \bar{g} = s\bar{d} - c\alpha \quad e = s\beta \quad \bar{d} = -c\beta$
 $\gamma = \max\{\|[\bar{g}, \beta]\|, e\} \quad c = \bar{g}/\gamma, \quad s = \beta/\gamma, \quad \phi = c\bar{\phi}, \quad \bar{\phi} = s\bar{\phi}$
 $w_1 = w_2, \quad w_2 = w$
 $w = (v - e_0w_1 - \delta w_2)\gamma^{-1}$
 $\mathbf{g} = \mathbf{Y}(\mathbf{Y}^T\mathcal{A}\mathbf{Y})^{-1}\mathbf{Y}^T\mathcal{A}w\phi$
 $u = u - \mathbf{g} + \phi w$
 $\zeta = \chi_1/\gamma, \quad \chi_1 = \chi_2 - \delta z, \quad \chi_2 = -e\zeta$
 Check preconditioned residual norm $(\bar{\phi})$ for convergence
 end

4. Variable viscosity and clustering effect. In this section we consider the particular example of the Stokes type problem with variable viscosity (1.1) and discuss why outliers may occur in the spectrum of $BA^{-1}B^TS^{-1}$. Numerical examples in section 5 show that the scenario with few outliers and a well clustered remainder of $\text{spec}(BA^{-1}B^TS^{-1})$ is obtained in practice. Thus assume conforming LBB-stable finite element spaces $\mathbb{V}_h \subset \mathbf{H}_0^1(\Omega)$ and $\mathbb{Q}_h \subset L^2(\Omega)$ for velocity and pressure are employed. Let $\{\phi_i\}_{1 \leq i \leq n}$ and $\{\psi_j\}_{1 \leq j \leq m}$ be nodal bases of \mathbb{V}_h and \mathbb{Q}_h , respectively. Define the matrices $A = \{A_{i,j}\} \in \mathbb{R}^{n \times n}$, $B = \{B_{i,j}\} \in \mathbb{R}^{m \times n}$, and $S = \{S_{i,j}\} \in \mathbb{R}^{m \times m}$ with

$$A_{i,j} = (\nu \mathbf{D}\phi_j, \mathbf{D}\phi_i), \quad B_{i,j} = -(\text{div } \phi_j, \psi_i), \quad S_{i,j} = (\nu^{-1}\psi_j, \psi_i).$$

Here and further (\cdot, \cdot) denotes the $L^2(\Omega)$ scalar product.

Due to the relation $\langle BA^{-1}B^T y, y \rangle = \sup_{x \in \mathbb{R}^n} \frac{\langle Bx, y \rangle^2}{\langle Ax, x \rangle}$, the bounds on the eigenvalues of preconditioned Schur complement $BA^{-1}B^TS^{-1}$ are given by the constants c_{\min}^2 and c_{\max}^2 from

$$c_{\min}^2 \langle Sy, y \rangle \leq \sup_{x \in \mathbb{R}^n} \frac{\langle Bx, y \rangle^2}{\langle Ax, x \rangle} \leq c_{\max}^2 \langle Sy, y \rangle \quad \forall y \in \mathbb{R}^m. \quad (4.1)$$

These relations can be rewritten as

$$c_{\min} \|q_h\| \leq \sup_{\mathbf{v}_h \in \mathbb{V}_h} \frac{(\text{div } \mathbf{v}_h, q_h)}{\|\nu^{\frac{1}{2}} \mathbf{D}\mathbf{v}_h\|} \leq c_{\max} \|q_h\| \quad \forall q_h \in \mathbb{Q}_h. \quad (4.2)$$

One easily finds $c_{\min} = 0$ and using Cauchy inequality $c_{\max} = d$. If $\nu = \text{const}$ and one considers only such $q_h \in \mathbb{Q}_h$ in (4.2) that $\int_{\Omega} q_h d\mathbf{x} = 0$, then $c_{\min} \geq c_{\text{lb}} > 0$ with some h -independent constant c_{lb} for finite elements satisfying the LBB stability condition [5]; here h denotes a mesh-size parameter. Hence, for the variable viscosity case a similar result easily follows with $c_{\min}^2 \geq \nu_{\min} \nu_{\max}^{-1} c_{\text{lb}}^2 > 0$. In practice, however, the ratio of viscosity variation $\nu_{\min}^{-1} \nu_{\max}$ can be very large leading to a poor spectrum estimate. A better insight into the spectrum properties can be gained at the continuous level, and it is based on the following result from [11]:

Assume ν is sufficiently smooth and $\partial\Omega$ is sufficiently regular, then the estimate

$$c_\nu \|\nu^{-\frac{1}{2}} q\| \leq \sup_{\mathbf{v} \in \mathbf{H}_0^1(\Omega)} \frac{(q, \operatorname{div} \mathbf{v})}{\|\nu^{\frac{1}{2}} \mathbf{D}\mathbf{v}\|}, \quad (4.3)$$

holds for any $q \in L^2(\Omega)$ such that

$$(q, \nu^{-1}) = (q, \nu^{-\frac{1}{2}}) = 0, \quad (4.4)$$

with

$$\begin{aligned} d = 2 : \quad c_\nu &= c_0(1 + c \|\nu^{\frac{1}{2}}\|_{L^k} \|\nabla \nu^{-\frac{1}{2}}\|_{L^r}) \quad \forall k > 2, r > 2k(k-2)^{-1} \\ d = 3 : \quad c_\nu &= c_0(1 + c \|\nu^{\frac{1}{2}}\|_{L^k} \|\nabla \nu^{-\frac{1}{2}}\|_{L^r}) \quad \forall k > 3, r = 3k(k-3)^{-1} \end{aligned}$$

Here constants c_0 and c depend only on Ω and possibly on k, r , cf. [11].

The result in (4.3) is the continuous counterpart of the lower bound in (4.2). Thus for LBB stable discretizations one may expect that a lower bound in (4.1) holds with c_{\min} exhibiting similar dependence on (the norms of) ν as c_ν . In general, this leads to a better lower bound (much better in some cases, see further discussion) than those given by $\nu_{\min} \nu_{\max}^{-1} c_{\text{lbb}}^2$. The side effect is, however, that *two* orthogonality conditions (cf. (4.4)) have to be satisfied by the pressure function. By the Courant-Fischer representation theorem the restriction of the estimate to a subspace of co-dimension 2 means that two outliers (one eventually equals 0) can occur in $\operatorname{spec}(BA^{-1}B^T S^{-1})$. Furthermore, if a decomposition of Ω into subdomains is given and one applies the result in (4.3) in every subdomain (the resulting constant is the minimum of corresponding constants in subdomains, see Lemma 3.4 in [11]) then the number of the orthogonality conditions would be twice the number of subdomains. Hence the number of uncontrolled eigenvalues, i.e. possible outliers, increases accordingly.

We consider the saddle point system resulting from the discretization of the Bercovier-Engelman regularized model of the Bingham viscoplastic fluid [3, 4]. In this model, the effective viscosity depends on the rate of deformation tensor as

$$\nu(\mathbf{x}) = 2\mu + \frac{\tau_s}{\sqrt{\varepsilon^2 + |\mathbf{D}\mathbf{u}(\mathbf{x})|^2}} \quad (4.5)$$

with plastic viscosity and yield stress constants $\mu > 0$ and $\tau_s \geq 0$. For modeling reasons the regularization parameter $\varepsilon > 0$ should be small enough to ensure that the quasi-Newtonian fluid described by (1.1) and (4.5) well approximates the viscoplastic medium. If the problem is linearized (on every non-linear iteration or time step) by letting $\mathbf{u}(\mathbf{x})$ in (4.5) to be a known velocity field, then a stable discretization brings us to problem (1.2).

Now we can find bounds for eigenvalues of $BA^{-1}B^T S^{-1}$ for a particular example of viscoplastic Bingham flow in a 2D channel (one of the few viscoplastic flows with known analytical representation): Let $\mu = 1$, $\tau_s \in [0, \frac{1}{2}]$, $\Omega = (0, 1)^2$, and $\mathbf{u} = (u, v)$ with

$$u = \begin{cases} \frac{1}{8}(1 - 2\tau_s)^2 & \text{if } \frac{1}{2} - \tau_s \leq y \leq \frac{1}{2} + \tau_s, \\ \frac{1}{8}[(1 - 2\tau_s)^2 - (1 - 2\tau_s - 2y)^2] & \text{if } 0 \leq y < \frac{1}{2} - \tau_s, \\ \frac{1}{8}[(1 - 2\tau_s)^2 - (2y - 2\tau_s - 1)^2] & \text{if } 1 \geq y > \frac{1}{2} + \tau_s, \end{cases} \quad (4.6)$$

$$v = 0, \quad p = -x.$$

One can clearly indicate the rigid behavior of a fluid (a constantly moving kernel) for $\frac{1}{2} - \tau_s \leq y \leq \frac{1}{2} + \tau_s$ and a flow region for $y < \frac{1}{2} - \tau_s$ and $y > \frac{1}{2} + \tau_s$.

We substitute the velocity from (4.6) in (4.5), so the coefficient $\nu(\mathbf{x})$ is now given. One easily finds $\nu_{\min} = O(1)$, $\nu_{\max} = O(\varepsilon^{-1})$. Furthermore, we decompose Ω into three subdomains: Ω_1 equal to the rigid zone; Ω_2 and Ω_3 are two flow regions. As explained earlier, by estimating $\|\nu^{\frac{1}{2}}\|_{L^k}$ and $\|\nabla\nu^{-\frac{1}{2}}\|_{L^\infty}$ in each subdomain for the constant c_ν in (4.3) one gets $c_\nu \geq c(s)\varepsilon^{-s}$ for any $s > 0$ subject to six orthogonality conditions (two for each subdomain) for the pressure variable q . If we assume that a similar estimate is enjoyed by the constant from the discrete counterpart of (4.3), then the Courant-Fischer representation theorem gives

$$\mu_1 = 0, \quad c\varepsilon < \mu_2 \leq \mu_3 \leq \dots \leq \mu_m \leq d \quad \text{and} \quad c(s)\varepsilon^{-s} \leq \mu_7. \quad (4.7)$$

Thus the behavior of $\text{spec}(BA^{-1}B^T S^{-1})$ in this example becomes clearer: For small values of ε there can occur at most six small outliers, other eigenvalues are well-clustered. Numerical calculations in the next section show that estimate (4.7) can be still non-optimal – in practice the number of outliers is smaller, only 2 outliers are observed, while other eigenvalues are clustered and μ_3 stays well-separated from 0 as $\varepsilon \rightarrow 0$. Thus (4.7) implies that (2.1) holds with some $\ell < 7$ and the result of Theorem 2.5 can be applied.

5. Experimental evidence. In this section, we show results of few numerical experiments for the variable viscosity problem described in the previous section. The goal of these experiments is to illustrate the analysis of the paper and to report on the performance of the augmented method. For the discretization we apply the finite element method with isoP2-P1 elements for the velocity-pressure spaces $\mathbb{V}_h\text{-}\mathbb{Q}_h$. This pair of spaces satisfies the LBB stability condition. The discretization is done in $\Omega = (0, 1)^2$ using uniform triangulation with mesh-size h .

TABLE 5.1
Eigenvalues of $BA^{-1}B^T S^{-1}$ and of AP^{-1} .

ε	μ_1	μ_2	μ_3	μ_{\max}	δ	$\lambda_{\min}(AP^{-1})$	$\lambda_{\max}(AP^{-1})$
10^{-4}	0	$7.543 \cdot 10^{-3}$	$4.456 \cdot 10^{-2}$	1.687	10^{-3}	0.30768	1.435
					10^{-2}	0.06342	1.812
10^{-5}	0	$7.725 \cdot 10^{-4}$	$4.260 \cdot 10^{-2}$	1.494	10^{-3}	0.31494	1.428
					10^{-2}	0.06412	1.753

TABLE 5.2
Eigenvalues of AP^{-1} .

ε	δ	λ_{\min}	λ_{m-2}	λ_{m-1}	λ_m	λ_{m+1}	λ_{\max}
10^{-4}	10^{-3}	-0.860	-0.0427	-0.00739	0	0.36043	2.043
	10^{-2}	-0.785	-0.0423	-0.00693	0	0.0820	2.357
10^{-5}	10^{-3}	-0.791	-0.0409	$-7.7 \cdot 10^{-4}$	0	0.35277	2.021
	10^{-2}	-0.712	-0.0406	$-7.65 \cdot 10^{-4}$	0	0.07565	2.267

First, we aim to confirm the existence of the outliers in the spectrum of the pre-conditioned Schur complement matrix for the example of the regularized Bingham flow in the channel from the previous section for sufficiently small values of parameter

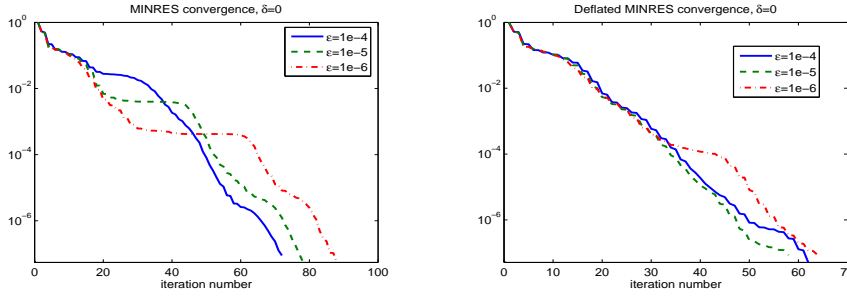


FIG. 5.1. Convergence histories for preconditioned MINRES with and without deflation for different values of the regularization parameter ε .

ε . Here and further we set $\tau = 0.3$ and consider two grids: The coarse one corresponds to $h = \frac{1}{16}$ resulting in $n = 1922$, $m = 289$, and the fine grid corresponds to $h = \frac{1}{32}$ resulting in $n = 7938$, $m = 1089$. Few smallest and the largest $\mu \in \text{sp}(BA^{-1}B^TS^{-1})$ are shown in Table 5.1 for $h = \frac{1}{16}$ (similar values were found for the finer mesh). Although up to six outliers are allowed by the analysis of the previous section, only two occur in practice. The preconditioner for the velocity block is defined through the Matlab incomplete Cholesky (IC) routine `cholinc(A, δ)`. The parameter δ specifies the fill-in of the Cholesky decomposition factors. We use $\delta \in \{0, 10^{-3}, 10^{-2}\}$, where $\delta = 0$ corresponds to the exact factorization. The preconditioning quality for $\delta \in \{10^{-3}, 10^{-2}\}$ can be assessed by inspecting the extreme eigenvalues of AP^{-1} in Table 5.1. The resulting distribution of the eigenvalues of the preconditioned coupled system \mathcal{AP}^{-1} is shown in Table 5.2.

The presence of the outliers may cause the stagnation period in the convergence history of a Krylov subspace method. Moreover, if the outlying values go to zero (as happens in our example) the stagnation phase may prolong. Both phenomena are well visible in Figure 5.1 (left). The stagnation periods form plateaus in the convergence plots for the MINRES method residual with various values of ε . Here and later on, the iterations were stopped once the ℓ_2 -norm of the initial residual was reduced by 10^7 . To cope with the influence of the outliers on the MINRES convergence we consider the augmentation strategy from section 3. The deflated MINRES needs (approximate) eigenvector corresponding to $\lambda_{m-1}(\mathcal{AP}^{-1})$. Although the influence of $\lambda_m(\mathcal{AP}^{-1}) = 0$ is formally avoided by choosing the initial vector from the appropriate subspace, one may also wish to include the corresponding eigenvector in the augmentation step to dampen the resurgence of that eigencomponent due to round-off. While the eigenvector for $\lambda_m(\mathcal{AP}^{-1})$ is easy to compute (see below), computing accurately the eigenvector $\{x_{m-1}, y_{m-1}\}^T$ for $\lambda_{m-1}(\mathcal{AP}^{-1})$ is expensive, in general.

Thus we look for a simple approximation to $\{x_{m-1}, y_{m-1}\}^T$. Observe the second pressure eigenfunction p_2 of the (left) preconditioned Schur complement in Figure 5.2, i.e. $S^{-1}BA^{-1}B^Tp_2 = \mu_2p_2$. The function is constant in flow regions and varies in the rigid region on the fluid, suggesting that the following simple approximation to p_2 could be appropriate:

$$\tilde{p}_2 = \begin{cases} 0 & \text{if } \frac{1}{2} - \tau_s \leq y \leq \frac{1}{2} + \tau_s, \\ 1 & \text{if } 0 \leq y < \frac{1}{2} - \tau_s, \\ -1 & \text{if } 1 \geq y > \frac{1}{2} + \tau_s. \end{cases}$$

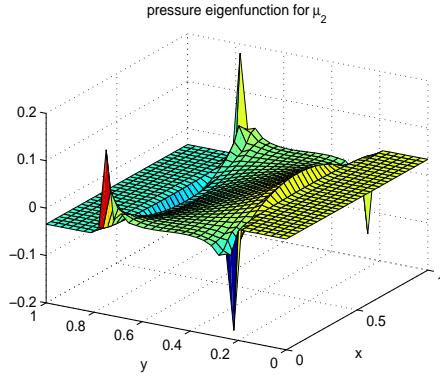


FIG. 5.2. Second pressure eigenfunction for $S^{-1}BA^{-1}B^T$.

Note that the particular scaling of p_2 is not important. With $u_2 = (\lambda_2 - 1)A^{-1}B^T p_2$ the vector $\{u_2, p_2\}^T$ is the eigenvector of $\mathcal{P}^{-1}\mathcal{A}$. Since in practice λ_2 is not known, though small, and A^{-1} is too expensive to apply exactly, we use

$$\{\tilde{u}_2, \tilde{p}_2\}^T \approx \{u_2, p_2\}^T, \quad \text{with} \quad \tilde{u}_2 = -P^{-1}B^T\tilde{p}_2$$

for augmented MINRES. We found this choice particularly effective. We conjecture that for more general viscoplastic flows the number of outliers matches the number of flow disconnected regions and the approximate eigenvectors can be built accordingly. Moreover, we note that the second pressure eigenfunction found for coarse grid problem looks very similar to the fine grid eigenfunction shown in figure 5.2. Thus in practice, it may be also recommended to take a computable coarse grid pressure eigenfunction as the approximation on a fine grid. The first augmentation eigenvector, $\{u_1, p_1\}^T = \{0, 1\}^T$, corresponds to the hydrostatic pressure mode. Figure 5.1 (right) shows convergence histories of deflated MINRES, where the approximate second eigenvector is used for the augmentation.

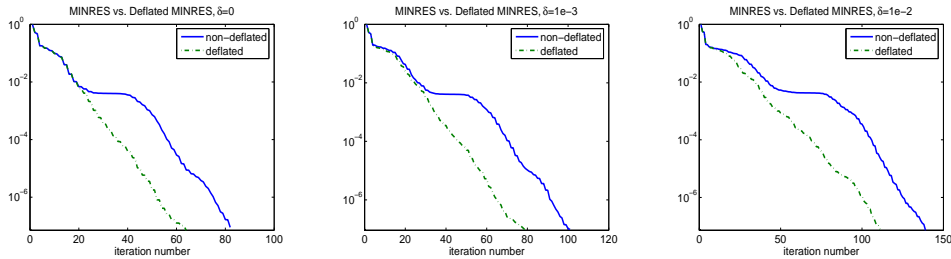


FIG. 5.3. Convergence histories for preconditioned MINRES with and without deflation for different values of the fill-in parameter δ in the IC preconditioner for the A block.

Figure 5.3 illustrates the influence of inexact A block preconditioning on the convergence of the standard and deflated MINRES method. As expected, larger δ , that is a poorer approximation to A , yields slower convergence. Nevertheless, the influence of small outliers and the cure by deflation can still be fully appreciated even for larger δ . Here we used the coarse mesh and approximate eigenvectors for augmentation. We also compute exact eigenvectors. It appears that the convergence

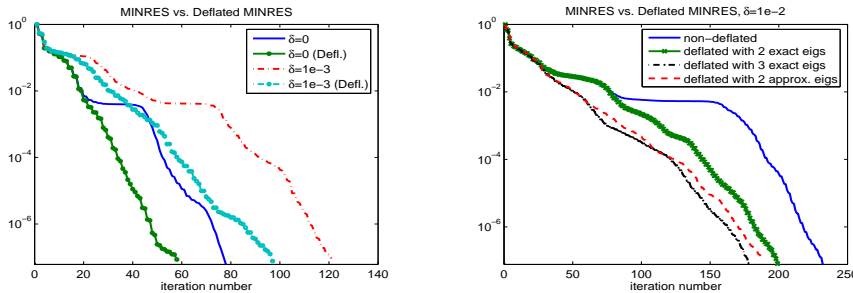


FIG. 5.4. Convergence histories for preconditioned MINRES with and without deflation for different values of δ in the IC preconditioner for the A block on a finer grid ($h = 1/32$). Left: deflated and non-deflated MINRES. Right: different numbers of deflation vectors.

curves of deflated MINRES with approximate and exact eigenvectors almost coincide in this example.

Finally, we repeat the same experiment with varying δ on the finer mesh. The results are shown in the left plot of Figure 5.4. Compared to the coarse grid, the following new phenomena are observed in this case: The Cholesky factorization with $\delta = 10^{-2}$ provides a too poor preconditioner for the A block and in addition to a small negative outlier a small positive eigenvalue emerges in the spectrum of $\mathcal{P}^{-1}\mathcal{A}$. In this case, the four eigenvalues smallest in magnitude are

$$-0.0405, -0.000747, 0, 0.0158.$$

The influence of the small positive eigenvalue becomes apparent in the convergence history. Thus the right plot in Figure 5.4 shows the convergence of the usual MINRES and deflated MINRES, where the augmentation is done (i) with two exact eigenvectors corresponding to λ_m and λ_{m-1} , (ii) with three exact eigenvectors corresponding to λ_m , λ_{m+1} and λ_{m-1} , and (iii) with two approximate eigenvectors corresponding to λ_m and λ_{m-1} . It appears that the use of approximate eigenvectors partially ameliorates the influence of both smallest positive and negative eigenvalues. We note that in practice, the typical choice of preconditioner for the A block is a multigrid method, see e.g. [6, 10]. Although less convenient for illustrative spectral analysis of this section, this choice leads to spectral bounds largely insensitive to the mesh size. In this case, the algorithm described in section 3 should be employed.

Numerical experiments were also performed using a different regularization model for the Bingham fluid from [17]. In that model, the effective viscosity is defined through

$$\nu(\mathbf{x}) = 2\mu + \tau_s \left(\frac{1 - \exp\left(-\frac{|\mathbf{D}\mathbf{u}(\mathbf{x})|}{\varepsilon}\right)}{|\mathbf{D}\mathbf{u}(\mathbf{x})|} \right),$$

where $\varepsilon > 0$ is the regularization parameter. Since all qualitative results of these experiments were the same, we do not report them here.

6. Conclusions. We showed that properties associated with clusters and outliers in the preconditioned Schur Complement matrix are favorably inherited by the spectrum of the preconditioned saddle point problem. To this end, we provided a quantitative description of the refined spectral intervals. We also proposed a strategy

to deal with the emerging outlying eigenvalues so that their delaying action is completely removed from the convergence history of an optimal Krylov subspace method. Numerical experiments fully confirmed our findings while displaying the good performance of the MINRES algorithm when approximate eigenvector information associated with the outlying eigenvalues is included.

REFERENCES

- [1] M. Benzi. Preconditioning techniques for large linear systems: a survey. *J. Comput. Phys.*, 182:418–477, 2002.
- [2] M. Benzi, G. H. Golub, and J. Liesen. Numerical solution of saddle point problems. *Acta Numerica*, 14:1–137, 2005.
- [3] M. Bercovier and M. Engelman. A finite element method for incompressible non-newtonian flows. *J. Comput. Phys.*, 36:313–326, 1980.
- [4] E. Bingham. *Fluidity and Plasticity*. McGraw-Hill Book Co., inc, 1922.
- [5] F. Brezzi and M. Fortin. *Mixed and Hybrid Finite Element Methods*. Springer-Verlag, New York, 1991.
- [6] C. Burstedde, O. Ghattas, G. Stadler, T. Tu, and L. C. Wilcox. Parallel scalable adjoint-based adaptive solution of variable-viscosity stokes flow problems. *Comput. Methods Appl. Mech. Engrg.*, 198:1691–1700, 2009.
- [7] S.-C. Choi. *Iterative Methods for Singular Linear Equations and Least-Squares Problems*. PhD thesis, Stanford University, 2006.
- [8] U. Christensen and H. Harder. 3-D convection with variable viscosity. *Geophys. J. Internat.*, 104:213–220, 2007.
- [9] A. Greenbaum. *Iterative methods for solving linear systems*. SIAM, PA, 1997.
- [10] P. P. Grinevich and M. A. Olshanskii. An iterative method for solving the regularized Bingham problem. *Numerical Methods and Programming*, 11:78–87, 2010.
- [11] P. P. Grinevich and M. A. Olshanskii. An iterative method for the Stokes-type problem with variable viscosity. *SIAM J. Sci. Comput.*, 31(5):3959–3978, 2009.
- [12] W. Hackbusch. *Multi-grid Methods and Applications*, volume 4. Springer Verlag, 1985.
- [13] R. A. Horn and C. R. Johnson. *Topics in Matrix Analysis*. Cambridge University Press, Cambridge, 1991.
- [14] J. Hron, J. Malék, J. Nečas, and K. R. Rajagopal. Numerical simulations and global existence of solutions of two-dimensional flows of fluids with pressure- and shear-dependent viscosities. *Math. Comput. Simulation*, 61:297–315, 2003.
- [15] M. A. Olshanskii and A. Reusken. Analysis of a Stokes interface problem. *Numer. Math.*, 103:129–149, 2006.
- [16] C. C. Paige and M. A. Saunders. Solution of sparse indefinite systems of linear equations. *SIAM J. Numer. Anal.*, 12(4):617–629, Sept. 1975.
- [17] T. C. Papanastasiou. Flows of materials with yield. *J. Rheol.*, 31:385–404, 1987.
- [18] A. Quarteroni and A. Valli. *Domain Decomposition Methods for Partial Differential Equations*. Oxford University Press, 1999.
- [19] M. ur Rehman, T. Geenen, C. Vuik, G. Segal, and S. P. MacLachlan. On iterative methods for the incompressible Stokes problem. *Int. J. Numer. Meth. Fluids*, DOI: 10.1002/fld.2235, 2010.
- [20] J. W. Ruge and K. Stüben. Algebraic multigrid. In *Multigrid Methods, Frontiers Appl. Math.* SIAM, Philadelphia, 1987.
- [21] T. Rusten and R. Winther. A preconditioned iterative method for saddle point problems. *SIAM J. Matrix Anal. Appl.*, 13(3):887–904, 1992.
- [22] Y. Saad. *Iterative methods for sparse linear systems*. SIAM, Society for Industrial and Applied Mathematics, 2nd edition, 2003.
- [23] Y. Saad, M. Yeung, J. Erhel, and F. Guyomarc’h. A deflated version of the Conjugate Gradient algorithm. *SIAM J. Sci. Comput.*, 21(1):1909–1926, 2000.
- [24] D. Silvester and A. Wathen. Fast iterative solution of stabilized Stokes systems part II: using general block preconditioners. *SIAM J. Numer. Anal.*, 31:1352–1367, 1994.
- [25] V. Simoncini and D. B. Szyld. Recent computational developments in Krylov subspace methods for linear systems. *J. Numerical Linear Algebra with Appl.*, 14(1):1–59, 2007.
- [26] G. W. Stewart and J-G. Sun. *Matrix Perturbation Theory*. Academic Press, 1990.
- [27] P. J. Tackley. Effects of strongly variable viscosity on three-dimensional compressible convection in planetary mantles. *J. Geophys. Res.*, 101:3311–3332, 1996.

- [28] A. Toselli and O. B. Widlund. *Domain Decomposition Methods - Algorithms and Theory*, volume 34 of *Springer Series in Computational Mathematics*. Springer Verlag, Heidelberg, 2004.